

Cite this: *Food Funct.*, 2025, **16**, 7796

# Nutritional targeting circulating eNAMPT attenuates NLRP3 inflammasome activation in alcoholic liver injury: therapeutic potential of nicotinamide riboside

Yujia Zhou,<sup>†a,c</sup> Xuye Lai,<sup>†a</sup> Nengzhi Pang,<sup>a,d</sup> Wenli Li,<sup>a</sup> Qiuyan Li,<sup>a</sup> Jie Pan,<sup>a</sup> Lei Pei,<sup>a</sup> Mingtao Chen,<sup>a</sup> Zhenfeng Zhang<sup>†b</sup>\* and Lili Yang<sup>†b</sup>\*<sup>a</sup>

Alcoholic liver disease (ALD) remains a major global health burden with limited effective nutritional strategies. We previously identified brown adipose tissue-derived extracellular nicotinamide phosphoribosyltransferase (eNAMPT) as a pathogenic factor in ALD, but the underlying mechanisms remained unclear. Here, we explored the role of eNAMPT on liver inflammation and evaluate the therapeutic potential of nicotinamide riboside (NR), a form of vitamin B3, as a potential nutritional intervention. We found that ethanol exposure significantly increased eNAMPT secretion from brown adipocytes (BACs) and elevated circulating eNAMPT levels in mice fed a chronic-plus-binge ethanol diet. RNA-seq analysis and rescue experiments showed that neutralizing eNAMPT reduced hepatic NLRP3 inflammasome activation and proinflammatory cytokine expression. In the co-culture experiment, BACs-derived eNAMPT induced NLRP3 inflammasome activation in hepatocytes and macrophages. However, this effect was abolished when eNAMPT was depleted from the conditioned medium of BACs. Furthermore, recombinant eNAMPT exerts a dose-dependent effect on the activation of the NLRP3 inflammasome in hepatocytes and macrophages. Importantly, oral supplementation with NR effectively suppressed ethanol-induced eNAMPT secretion and mitigated hepatic NLRP3 activation both *in vivo* and *in vitro*. The secretion of eNAMPT was inhibited when NAMPT was knocked down in BACs, thereby attenuating the anti-inflammatory effect of NR, indicating its protective effect is dependent on targeting eNAMPT secretion. Our findings reveal BACs-derived eNAMPT as a key mediator linking adipose–liver inflammation in ALD and support dietary NR as a promising intervention strategy by targeting eNAMPT.

Received 17th July 2025,  
Accepted 5th September 2025

DOI: 10.1039/d5fo03002a

rsc.li/food-function

## 1. Introduction

Alcoholic liver disease (ALD) has emerged as a major chronic liver disease in China, largely due to increased alcohol consump-

tion in recent years.<sup>1,2</sup> The rising burden of ALD has made it a significant public health concern, highlighting the urgent need for novel and effective therapeutic strategies.<sup>2–4</sup> The progression of ALD involves multiple pathogenic factors, including acetaldehyde toxicity, oxidative stress, and hepatic inflammation.<sup>5</sup> Recent studies have increasingly focused on the role of inter-organ communication,<sup>6</sup> particularly the crosstalk between adipose tissue and the liver, in regulating liver inflammation.<sup>7–9</sup> Extracellular nicotinamide phosphoribosyltransferase (eNAMPT), also known as pre-B colony-enhancing factor or visfatin, is a multifunctional protein secreted predominantly by adipocytes.<sup>10</sup> Although extensively studied, the physiological functions and regulatory mechanisms of eNAMPT secretion remain controversial.<sup>11</sup> Our previous work demonstrated that inhibition of eNAMPT release from brown adipose tissue (BAT) alleviated ethanol-induced liver injury, implicating eNAMPT as a potential upstream driver of hepatic pathology in ALD.<sup>12</sup> However, the precise mechanisms through which BAT-derived eNAMPT influences liver inflammation remain unclear.

<sup>a</sup>Department of Nutrition, Guangdong Provincial Key Laboratory of Food, Nutrition and Health, School of Public Health, Sun Yat-sen University, Guangzhou, Guangdong, 510080, China. E-mail: yangll7@mail.sysu.edu.cn

<sup>b</sup>Radiology Center; Translational Medicine Center; Guangzhou Key Laboratory for Research and Development of Nano-Biomedical Technology for Diagnosis and Therapy; Guangdong Provincial Education Department Key Laboratory of Nano-Immunoregulation Tumour Microenvironment; Central Laboratory, the Second Affiliated Hospital, Guangzhou Medical University, Guangzhou, Guangdong, China. E-mail: zhangzhf@gzhmu.edu.cn

<sup>c</sup>State Key Laboratory of Oncology in South China, Guangdong Provincial Clinical Research Center for Cancer, Sun Yat-sen University Cancer Center, Guangzhou, 510060, China

<sup>d</sup>Department of Nutrition and Food Hygiene, School of Public Health, Hainan Medical University, Haikou, Hainan, China

<sup>†</sup>These authors contributed equally.



eNAMPT acts as a pro-inflammatory cytokine and contributes to the pathogenesis of several inflammatory diseases.<sup>13–15</sup> The activation of the nucleotide-binding oligomerization domain-like receptor protein 3 (NLRP3) inflammasome plays a pivotal role in promoting immune cell infiltration and exacerbating liver inflammation.<sup>16,17</sup> In endothelial cells, eNAMPT has been shown to promote NLRP3 inflammasome activation and subsequent secretion of key pro-inflammatory cytokines such as IL-1 $\beta$  and TNF- $\alpha$ .<sup>13,18</sup> Despite these findings, the specific cellular source of eNAMPT during alcohol-related inflammation and its contribution to liver injury remain to be elucidated. We hypothesize that BAT-derived eNAMPT is a critical mediator of hepatic inflammation in ALD and that targeting its secretion could offer a novel preventive and therapeutic approach. eNAMPT secretion is modulated by cellular stress, nutrient availability, and inflammatory stimuli.<sup>11</sup> In light of the increasing emphasis on nutritional interventions in ALD management, we propose that dietary modulation of eNAMPT may represent a promising strategy. Nicotinamide riboside (NR), a natural dietary supplement and a form of vitamin B3 found in milk and beer,<sup>19</sup> has shown efficacy in mitigating ethanol-induced hepatic steatosis, as well as carbon tetrachloride-induced liver fibrosis in our previous studies.<sup>20,21</sup> However, whether NR can regulate eNAMPT secretion and influence alcohol-induced hepatic inflammation remains unknown.

This study investigates the role of BAT-derived eNAMPT in mediating hepatic NLRP3 inflammasome activation in ALD and evaluate the therapeutic potential of NR supplementation. We aim to provide mechanistic insights into the protective effects of NR and to identify eNAMPT as a promising therapeutic target for ALD by uncovering the role of the adipose–liver inflammatory axis and its modulation through nutritional intervention.

## 2. Materials and methods

### 2.1 Cell culture and treatment

The normal liver epithelial cell line AML12 (alpha mouse liver 12) was maintained in DMEM/F-12 (1 : 1) supplemented with insulin–transferrin–selenium–ethanolamine (ITS-X, 51500056; Thermo Scientific, MA, USA), 10% fetal bovine serum (Gibco, Carlsbad, CA, USA), and 1% penicillin–streptomycin, in a 5% CO<sub>2</sub> atmosphere at 37 °C. The murine macrophage cell line RAW 264.7, ectopically expressing ASC, was cultured in RPMI 1640 supplemented with 10% fetal bovine serum (Gibco, Carlsbad, CA, USA) and 1% penicillin–streptomycin, under identical conditions. Cells were treated with recombinant eNAMPT protein at concentrations of 5 ng mL<sup>-1</sup> and 10 ng mL<sup>-1</sup> (8424-VF-050; Bio-Techne, R&D Systems, Inc., Minnesota, USA) for 24 hours. Stromal vascular fraction cells (SVFs) were isolated from the subcutaneous fat of mice and differentiated into mature brown adipocytes *in vitro*, as previously described.<sup>22</sup> After treatment with NR (0.5 mmol L<sup>-1</sup>; ChromaDex, Irvine, CA, USA) for 96 hours together with

ethanol (100 mmol L<sup>-1</sup>; Aladdin, Shanghai, China) exposure, the mature brown adipocytes were harvested, and eNAMPT was removed from the medium through immunoprecipitation. The conditioned medium (CM) was subsequently cultured with AML12 cells and RAW 264.7 cells for an additional 24 hours.

### 2.2 Cell migration assay

Cells were seeded in a 6-well plate and grown to confluence. A sterile pipette tip was used to create a uniform scratch in the cell monolayer. After the scratch, the culture medium was removed, and the cells were washed with PBS to remove debris. Fresh medium with or without treatment recombinant eNAMPT protein at concentrations of 5 ng mL<sup>-1</sup> and 10 ng mL<sup>-1</sup> was added to the wells. The cells were incubated at 37 °C with 5% CO<sub>2</sub>, and images of the wound area were captured at designated time points (0 and 48 hours) using a phase-contrast microscope. The migration rate was quantified by measuring the distance of cell movement into the wound area, using Image J analysis software.

### 2.3 Immunoprecipitation

After ethanol treatment, brown adipocytes were incubated with NAMPT antibody (BETHLY, A300–372A, Texas, USA; 1 : 500) or normal IgG antibody (1 : 500) for 1 hour at 37 °C. Subsequently, 20  $\mu$ L of protein A/G plus agarose beads (Santa Cruz, Inc., CA, USA) was added, and the mixture was rotated overnight at 4 °C. Samples were then centrifuged at 1000g for 2 minutes at 4 °C. The supernatant was collected and utilized as the conditioned medium.

### 2.4 Western blot

Total protein was extracted from mouse livers or cultured cells using RIPA lysis buffer containing PMSF (Beyotime, Shanghai, China), followed by centrifugation at 14 000g for 20 minutes at 4 °C. Protein concentration in the supernatant was quantified using a BCA kit from Beyotime (Shanghai, China). Western blot analysis was conducted as previously described.<sup>21</sup> The following primary antibodies were employed: NAMPT (BETHLY, A300–372A, Texas, USA), IL-1 $\beta$  (CST, MA, USA), GAPDH (CST, MA, USA), tubulin (Abcam, Cambridge, UK), ACTIN (CST, MA, USA), ASC (CST, MA, USA), NLRP3 (Abcam, Cambridge, UK), Pro-caspase-1 (Proteintech, Rosemont, USA), and caspase-1 p20 (Santa Cruz, Inc., CA, USA).

To quantify eNAMPT protein concentration in the medium, 20  $\mu$ L of medium was combined with 5  $\mu$ L of 5 $\times$  SDS loading buffer and boiled at 95 °C for 10 minutes. For eNAMPT detection in serum, 2  $\mu$ L of serum was mixed with 98  $\mu$ L of RIPA buffer and then combined with 20  $\mu$ L of 5 $\times$  SDS loading buffer, followed by boiling at 95 °C for 10 minutes. Remaining procedures were conducted as described above. We provided the uncropped, full-length western blot images as SI.

### 2.5 Quantification of NR and NAD<sup>+</sup> levels

Cell samples were subjected to 400  $\mu$ L of 80% methanol (HPLC, Merck, Darmstadt, Germany) containing 20 nmol per L nevirapine per well, followed by collection by scraping the cells



into Eppendorf tubes. The samples were homogenized using a high-throughput tissue grinding instrument (Xinzhi, Co., Ltd, China). After centrifugation at 14 000g for 10 minutes at 4 °C, the supernatant was removed, dried in a rotary evaporator, and resuspended in 80 µL of 20% acetonitrile. Following centrifugation at 14 000g for 35 minutes at 4 °C, the supernatant was transferred to the liner of an Agilent sample bottle for analysis. A Hypercarb column (100 × 2.1 mm, 3 µm, Thermo Fisher Scientific, MA, USA) was employed as previously described.<sup>21</sup> The aqueous phase contained 7.5 mmol L<sup>-1</sup> ammonium acetate and 0.5% ammonia, while the acetonitrile organic phase contained 0.5% ammonia. The injection volume was 3 µL, with a flow rate of 0.15 mL min<sup>-1</sup>. NR and NAD<sup>+</sup> levels were quantified using an ultra-performance liquid chromatography tandem quadrupole time-of-flight mass spectrometer (UPLC-QTOF, 1290Infinity/6538, Agilent, Palo Alto, CA, USA) and normalized using nevirapine as an internal reference.

## 2.6 Animal models

Eight-week-old male C57BL/6 mice were obtained from the Guangdong Medical Laboratory Animal Center. All animal experiments were approved by the Animal Ethics Committee of Sun Yat-sen University (2021002133, Guangzhou, China). The mouse model of alcoholic liver injury (NIAAA) was established as previously described.<sup>23</sup> Control mice were acclimatized for 5 days on a Lieber-Decarli control liquid diet (TP4030C; TROPIC Animal Feed High-tech Co., Ltd, Nantong, China). For the ethanol-fed group, the control diet was gradually replaced with a 5% Lieber-Decarli ethanol liquid diet (TP4030D; TROPIC Animal Feed High-tech Co., Ltd, Nantong, China), with ethanol concentrations ranging from 1% to 4% from days 2 to 5. Mice were maintained on the 5% Lieber-Decarli ethanol liquid diet for 10 days, while control mice were pair-fed with the Lieber-Decarli control diet. On the morning of day 11, the ethanol-fed mice were gavaged with 5 g per kg body weight of alcohol, while control mice received an equicaloric maltodextrin solution. Mice were sacrificed 9 hours after gavage.

For eNAMPT neutralization studies, 8-week-old male mice were randomly assigned to three groups: the control group ( $n = 6$ ), the ethanol (EtOH) group ( $n = 9$ ), and the EtOH + anti-NAMPT group ( $n = 9$ ). Mice in the EtOH + anti-NAMPT group were administered an intraperitoneal injection of 0.4 mg kg<sup>-1</sup> of NAMPT antibody (BETHLY, A300-372A, Texas, USA) every three days for 10 days. The control and EtOH groups received equivalent volumes of normal IgG antibody (CST, #2729, Massachusetts, USA).

For NAD supplementation, 8-week-old male mice were similarly divided into three groups: the control group ( $n = 6$ ), the EtOH group ( $n = 9$ ), and the EtOH + NR group ( $n = 9$ ). Mice in

the EtOH + NR group were administered 400 mg per kg body weight of NR by gavage daily, while control and EtOH groups received an equal volume of saline *via* gavage.

## 2.7 RNA-seq analysis

Total RNA was extracted from mouse livers, and RNA-seq analysis was performed on the BGI Genomics platform (BGI-Shenzhen, China). Clean reads were mapped to the reference genome (species: *Mus musculus*; source: NCBI; reference genome version: Gcf\_000001635.26\_grem38.p6) using HISAT2. Analysis results were uploaded to the Dr Tom multi-omics data mining system (Shenzhen, BGI) for gene quantification, differential gene screening, and statistical analysis of differentially expressed genes (DEGs).

## 2.8 Knockdown of NAMPT in BACs

Post-confluent mature brown adipocytes in 12-well plates were divided into si-NAMPT group and si-NC group (siRNA sequences are listed in Table 1). siRNA was diluted in Opti-MEM (Gibco, #31985070, Carlsbad, CA, USA), followed by addition of RNAFit transfection reagent (GeneCopoeia, #EF013). The mixture was vortexed thoroughly and incubated at room temperature for 10 to 20 minutes. During transfection complex formation, 0.8 mL of pre-warmed DMEM was added to each well. The transfection complex was then introduced into the wells and gently mixed, achieving a final volume of 1 mL per well with 50 nM siRNA and 2 µL RNAFit reagent. After 6-hour incubation at 37 °C with 5% CO<sub>2</sub>, the si-NAMPT and si-NC groups were further subdivided into four experimental subgroups: CON (control), NR (0.5 mmol L<sup>-1</sup> nicotinamide riboside), EtOH (100 mmol L<sup>-1</sup>, Aladdin), and EtOH + NR groups. All groups received DMEM supplemented with 1% penicillin–streptomycin. The humidified atmosphere of EtOH group and EtOH + NR group was maintained by placing 6 mL of 95% ethanol in 1 L sterile water in the incubator chamber. Cells were incubated for 48 hours at 37 °C with 5% CO<sub>2</sub>. After the incubation period, the transfection protocol and pharmacological interventions were repeated, after which cells and conditioned medium were harvested for subsequent analyses.

## 2.9 Quantitative real-time PCR

Total RNA was extracted from mouse livers using TRIzol. cDNA was synthesized from total RNA employing a DNA removal and reverse transcription kit (RR047A, TAKARA, Invitrogen, Carlsbad, CA, USA). Real-time PCR was conducted using TB Green® premix Ex Taq II (RR820A, TAKARA, Invitrogen, Carlsbad, CA, USA) on a Vii7 System (ABI, Carlsbad, USA) to obtain CT values, with 2<sup>-ΔΔCt</sup> values utilized for analyzing relative mRNA levels. β-Actin served as a reference gene. RT-

**Table 1** Sequences of the siRNA

| Gene    | Species | Forward                  | Reverse                  |
|---------|---------|--------------------------|--------------------------|
| siNAMPT | Mouse   | UCAGCGAUAGCUAUGACAUUU TT | AAAUGUCAUAGCUAUCGCUGA TT |
| si-NC   | Mouse   | UUCUCCGAACGUGUCACGU TT   | UUCUCCGAACGUGUCACGU TT   |



Table 2 Sequences of the RT-qPCR primers

| Gene           | Species | Forward primer          | Reverse primer          |
|----------------|---------|-------------------------|-------------------------|
| IL-1 $\beta$   | Mouse   | GCAACTGTTTCCTGAACTCAACT | ATCTTTTGGGGTCCGTCAACT   |
| TNF $\alpha$   | Mouse   | CCGGGAGAAGAGGGATAGCTT   | TCGGACAGTCACTCACCAAGT   |
| SAA1           | Mouse   | CAGATCTGCCAGGAGACAC     | TCATGTCAGTGTAGGCTCGC    |
| Cxcl1          | Mouse   | CTGGGATTCACCTCAAGAACATC | CAGGGTCAAGGCAAGCCTC     |
| Cxcl2          | Mouse   | CCAACCACCAGGCTACAGG     | GCGTCACACTCAAGCTCTG     |
| CD206          | Mouse   | CTCTGTTCAGCTATTGGACGC   | CGGAATTTCTGGGATTCAGCTTC |
| CD80           | Mouse   | ACCCCCAACATAACTGAGTCT   | TTCCAACCAAGAGAAGCGAGG   |
| IL-12          | Mouse   | CTGTGCCTTGGTAGCATCTATG  | GCAGAGTCTCGCCATTATGATTC |
| IL-10          | Mouse   | GCTCTTACTGACTGGCATGAG   | CGCAGCTCTAGGAGCATGTG    |
| TGF $\beta$    | Mouse   | CTCCCGTGGCTTCTAGTGC     | GCCTTAGTTTGGACAGGATCTG  |
| $\beta$ -Actin | Mouse   | GTGGTGGTGAAGCTGTAGCC    | AGCCATGTACGTAGCCATCC    |

qPCR analysis was performed as previously described.<sup>21</sup> The primer sequences used in this study are presented in Table 2.

### 2.10 Statistical analysis

All results are expressed as mean (SD). Comparisons among multiple groups were analyzed using one-way ANOVA followed by Bonferroni's *post hoc* multiple comparison test to determine statistical significance. Comparisons between two experimental groups were assessed using Student's *t*-test. A *p*-value of <0.05 was considered statistically significant. All analyses were conducted using GraphPad Prism 9.0.0 (GraphPad Software, San Diego, CA, USA).

## 3. Results

### 3.1 Ethanol increases eNAMPT secretion from brown adipocytes

eNAMPT is an adipokine secreted by adipocytes.<sup>24</sup> We observed that ethanol intake significantly increased the levels of eNAMPT in the serum of mice (Fig. 1A–C). Histological analysis revealed that ethanol intake induced lipid accumulation and elevated NAMPT expression in BAT (Fig. 1D–G). To investigate whether the increased circulating eNAMPT is a result of alcohol-induced secretion from brown adipocytes, we analyzed eNAMPT secretion during adipocyte differentiation *in vitro* from preadipocytes to mature brown adipocytes. A gradual increase in eNAMPT secretion was observed, indicating that brown adipocytes serve as a source of eNAMPT (Fig. 1H and I). Following 96 hours of ethanol treatment, we measured eNAMPT levels in the culture media by western blot. The results showed that ethanol significantly increased NAMPT expression in brown adipocytes and enhanced the secretion of eNAMPT into the culture supernatant (Fig. 1J). In contrast, ethanol treatment did not alter NAMPT expression or eNAMPT secretion in white adipocytes (Fig. S1A–D), are the primary mediators of ethanol-induced eNAMPT secretion.

### 3.2 Neutralizing eNAMPT protects against alcohol-induced liver NLRP3 inflammasome activation in mice

To investigate the role of eNAMPT in alcoholic liver injury, we neutralized circulating eNAMPT using a polyclonal antibody

against NAMPT (anti-NAMPT) in a NIAAA mouse model of chronic and binge ethanol feeding. Anti-NAMPT was administered *via* intraperitoneal injection every three days (Fig. 2A). Compared to control mice, ethanol-fed mice exhibited significantly elevated eNAMPT protein levels in serum (Fig. 2B and C). As anticipated, treatment of ethanol-fed mice with anti-NAMPT significantly reduced serum eNAMPT levels (Fig. 2B and C), indicating that neutralizing eNAMPT markedly decreased circulating eNAMPT levels. Additionally, anti-NAMPT treatment significantly reduced serum AST and ALT levels in ethanol-fed mice (Fig. 2D).

To further explore the mechanism of eNAMPT in alcoholic liver injury, we performed transcriptome analysis *via* RNA sequencing on liver tissue from the different groups. Statistical analyses of differentially expressed genes (DEGs) revealed significant upregulation of genes encoding key acute-phase proteins associated with inflammation, including *Saa1*, *Saa2*, and *Orm2*, in the ethanol-fed group compared to the control group (Fig. 2E). However, anti-NAMPT treatment significantly downregulated the expression of these genes (Fig. 2E). A volcano plot further illustrated that *Saa1*, *Saa2*, and *Cxcl1* genes were significantly downregulated in the anti-NAMPT treatment group compared to the ethanol group (Fig. 2F). RNA-seq data suggested that neutralizing circulating eNAMPT mitigates the inflammatory response and reduces the expression of pro-inflammatory cytokines in the liver. We validated these findings using quantitative real-time PCR, revealing that mRNA expression levels of pro-inflammatory factors (*Saa1*, *Cxcl1*, *Cxcl2*, *IL-1 $\beta$* , and *Tnf- $\alpha$* ) in ethanol-fed mice (Fig. 2G). Treatment with anti-NAMPT decreased the mRNA expression of these hepatic proinflammatory cytokines (Fig. 2G).

The NLRP3 inflammasome, a multiprotein complex composed of NLRP3, ASC, and pro-caspase-1, is activated in response to various stimuli.<sup>25</sup> Upon activation, the NLRP3 inflammasome cleaves and activates caspase-1, which subsequently cleaves pro-IL-1 $\beta$  into its mature form, IL-1 $\beta$ . We found that ethanol increased the protein expression of NLRP3, activated caspase-1, and mature IL-1 $\beta$  in the liver, suggesting that ethanol consumption induced NLRP3 inflammasome activation (Fig. 2H and I). However, anti-NAMPT treatment significantly reduced the expression of NLRP3, caspase-1, and mature IL-1 $\beta$  in the liver, thereby inhibiting NLRP3 inflamma-



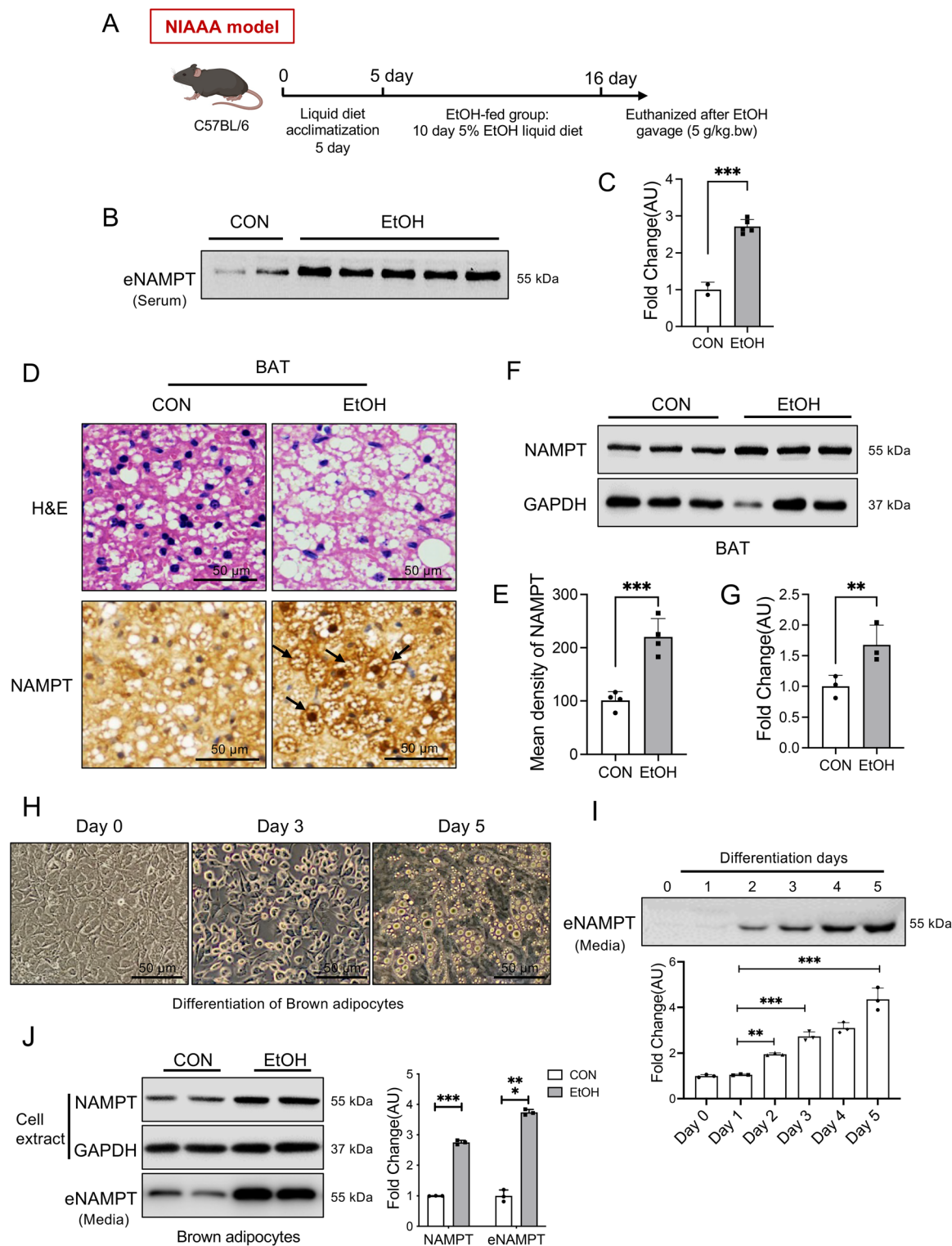


**Fig. 1** Ethanol increases eNAMPT secretion from brown adipocytes. (A) Schematic of the experimental design of mice were treated with chronic-plus-binge ethanol feeding for 16 days. (B) Serum levels of eNAMPT were measured by western blot ( $n = 2-5$  per group), (C) results were expressed as fold changes of control. (D) H&E stain and immunohistochemical staining of NAMPT in mouse BAT. (E) Quantitative analysis of immunohistochemistry. (F) The protein levels of NAMPT in BAT were measured by western blot, (G) results were expressed as fold changes of control. (H and I) Isolation stromal vascular fraction cells (SVFs) were differentiated to mature brown adipocytes, (H) images showed the gradually differentiation and maturation of brown adipocytes as time went by; (I) western blot analysis of eNAMPT in media, results were expressed as fold changes of control. (J) Brown adipocytes were treated with or without EtOH ( $100 \text{ mmol L}^{-1}$ ) for 96 h, western blot analysis of eNAMPT in media, results were expressed as fold changes of control. Data are presented as mean (SD).  $n = 2-5$  per group; \* $p < 0.05$ , \*\* $p < 0.01$ , \*\*\* $p < 0.001$ , \*\*\*\* $p < 0.0001$ .



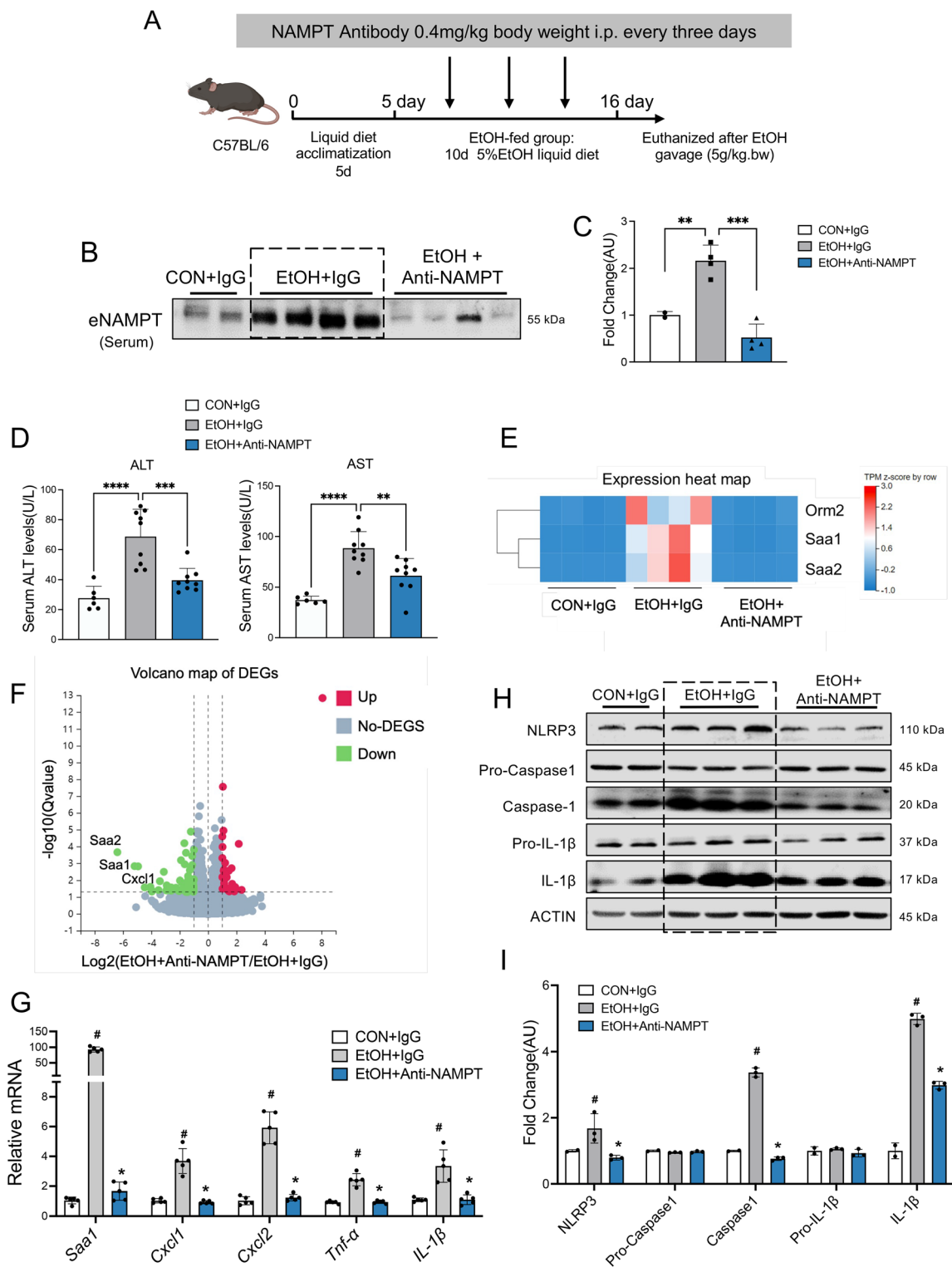


**Fig. 2** Neutralizing eNAMPT protects against alcohol-induced liver NLRP3 inflammasome activation in mice. (A) Schematic of the experimental design of mice were treated with chronic-plus-binge ethanol feeding and NAMPT neutralizing antibody treatment for 16 days. (B) Serum levels of eNAMPT were measured by western blot, (C) results were expressed as fold changes of control. (D) Serum levels of AST and ALT were assessed. (E and F) The mRNA-seq sequencing in mice liver, (E) expression heat map and (F) volcano plot of differentially expressed genes (DEGs). (G) Hepatic mRNA levels of pro-inflammatory or anti-inflammatory cytokine genes were measured via qRT-PCR. (H) Hepatic protein levels of NLRP3 inflammasome were measured by western blot, (I) results were expressed as fold changes of control. Data are presented as mean (SD).  $n = 6-9$  per group; \*\* $p < 0.01$ , \*\*\* $p < 0.001$ , \*\*\*\* $p < 0.0001$ , \* $p < 0.05$  compared with the EtOH group; # $p < 0.05$  compared with the control group.



some activation (Fig. 2H and I). These results suggest that blocking eNAMPT signaling significantly alleviates ethanol-induced NLRP3 inflammasome activation and the associated inflammatory response in the liver, indicating eNAMPT may serve as a potential therapeutic target for alcohol-induced hepatic inflammation.

### 3.3 BACs-derived eNAMPT induces NLRP3 inflammasome activation in hepatocytes and macrophages

To determine whether BACs-derived eNAMPT secretion regulates NLRP3 inflammasome activation in liver, we neutralized eNAMPT in the culture medium (CM) of brown adipocytes through immunoprecipitation and transferred this CM to culture AML12 and RAW 264.7 cells (Fig. 3A). Western blot analysis confirmed that eNAMPT levels in the CM from the ethanol treatment group were significantly reduced following neutralization (Fig. 3B and C). After culturing AML12 and RAW 264.7 cells with the CM for 24 hours, we assessed the expression of NLRP3 inflammasome-related proteins by western blot. We found that CM from ethanol-treated AML12 cells increased the protein expression of NLRP3, ASC, caspase-1, and mature IL-1 $\beta$  (Fig. 3D and E). However, neutralization of eNAMPT in the CM significantly inhibited these protein expressions (Fig. 3D and E), indicating that the neutralization of eNAMPT led to the inactivation of the NLRP3 inflammasome and a reduction in IL-1 $\beta$  production. Similarly, CM from ethanol-treated RAW 264.7 cells induced NLRP3 inflammasome activation, which was suppressed by neutralizing eNAMPT in the CM (Fig. 3F and G). These results suggest that BACs-derived eNAMPT secretion regulates NLRP3 inflammasome activation in both hepatocytes and macrophages.

### 3.4 Recombinant eNAMPT activates NLRP3 inflammasome in hepatocytes and macrophages

To confirm the proinflammatory effects of eNAMPT, we incubated AML12 and RAW 264.7 cells with two concentrations of recombinant eNAMPT (5 ng mL<sup>-1</sup> and 10 ng mL<sup>-1</sup>) for 24 hours. Our results demonstrated that eNAMPT treatment dose-dependently increased the protein expression of NLRP3 and ASC in AML12 cells (Fig. 4A and B). Additionally, the expression of the activated form of caspase-1 and mature IL-1 $\beta$  was significantly elevated in a dose-dependent manner following eNAMPT treatment (Fig. 4A and B), indicating that eNAMPT induces NLRP3 inflammasome activation in AML12 cells. Similarly, recombinant eNAMPT treatment increased NLRP3 and ASC protein expression and induced the cleavage of procaspase-1 to caspase-1, as well as the cleavage of pro-IL-1 $\beta$  to mature IL-1 $\beta$  in RAW 264.7 cells (Fig. 4C and D). To eliminate the possibility of LPS contamination, we heat-inactivated the recombinant eNAMPT by incubating it at 56 °C for 30 minutes. The results showed that heat inactivation inhibited eNAMPT-induced NLRP3 activation (Fig. S2), suggesting that the role of eNAMPT in NLRP3 inflammasome activation was not associated with LPS contamination. Furthermore, eNAMPT treatment increased the migration of RAW 264.7 cells in a dose-dependent manner (Fig. 4E and F). Cell morphologi-

cal analysis showed that RAW 264.7 cells changed from round to spindle-shaped following eNAMPT treatment, indicating macrophage polarization (Fig. 4G and H). In addition, our results showed that eNAMPT is localized on the macrophage membrane (Fig. S3) and promoted it to M1 polarization (Fig. S4). These findings confirm that eNAMPT can activate NLRP3 inflammasome in hepatocytes and macrophages, further supporting its proinflammatory effects.

### 3.5 NR supplementation protects against alcohol-induced liver NLRP3 inflammasome activation and decreases circulating eNAMPT levels in mice

Given the significant role of eNAMPT in liver inflammation, we sought a safer, more implementable strategy to target eNAMPT for potential clinical application. We treated the NIAAA model mice with NR (400 mg per kg bw) for 16 days (Fig. 5A). NR supplementation reduced ethanol-induced lipid accumulation and elevated NAMPT expression in BAT (Fig. 5B and C). Additionally, NR supplementation significantly inhibited the ethanol-induced increase in serum eNAMPT concentration (Fig. 5D and E), and reduced serum AST and ALT levels in ethanol-fed mice (Fig. 5F). Moreover, NR supplementation significantly reduced the protein expression levels of activated caspase-1, mature IL-1 $\beta$ , and NLRP3 in the liver, indicating that NR treatment inhibits ethanol-induced NLRP3 inflammasome activation (Fig. 5G and H). We also measured the expression of proinflammatory cytokines in the liver. Ethanol treatment elevated the hepatic mRNA levels of pro-inflammatory factors, but NR treatment inhibited this ethanol-induced pro-inflammatory response (Fig. 5I). These results suggest that NR supplementation may represent a promising therapeutic approach for ethanol-induced hepatic inflammation by targeting eNAMPT.

### 3.6 NR supplementation inhibits ethanol-induced eNAMPT secretion from BACs

To determine whether NR directly regulates eNAMPT secretion to mitigate liver inflammation, we incubated mature brown adipocytes with ethanol, with or without NR supplementation, for 96 hours. We then collected the culture medium (CM) and transferred them to AML12 and RAW 264.7 cell cultures for 24 hours (Fig. 6A). Ethanol exposure increased intracellular NAMPT expression and decreased NAD levels, whereas NR supplementation reversed these changes by reducing NAMPT expression and restoring NAD levels (Fig. S5). As expected, NR supplementation effectively inhibited ethanol-induced eNAMPT secretion from brown adipocytes (Fig. 6B and C). We measured the levels of NR in the CM. NR was completely metabolized by brown adipocytes after 96 hours, and no trace of NR was detected in the CM (Fig. S6). This confirmed that the effects of the CM on hepatocytes and macrophages were due to the secretions of brown adipocytes, not residual NR. Subsequently, we assessed the expression of NLRP3 inflammasome-related proteins by western blot. As anticipated, treatment with CM from ethanol-treated adipocytes increased the expression levels of NLRP3 and ASC, as well as the activation



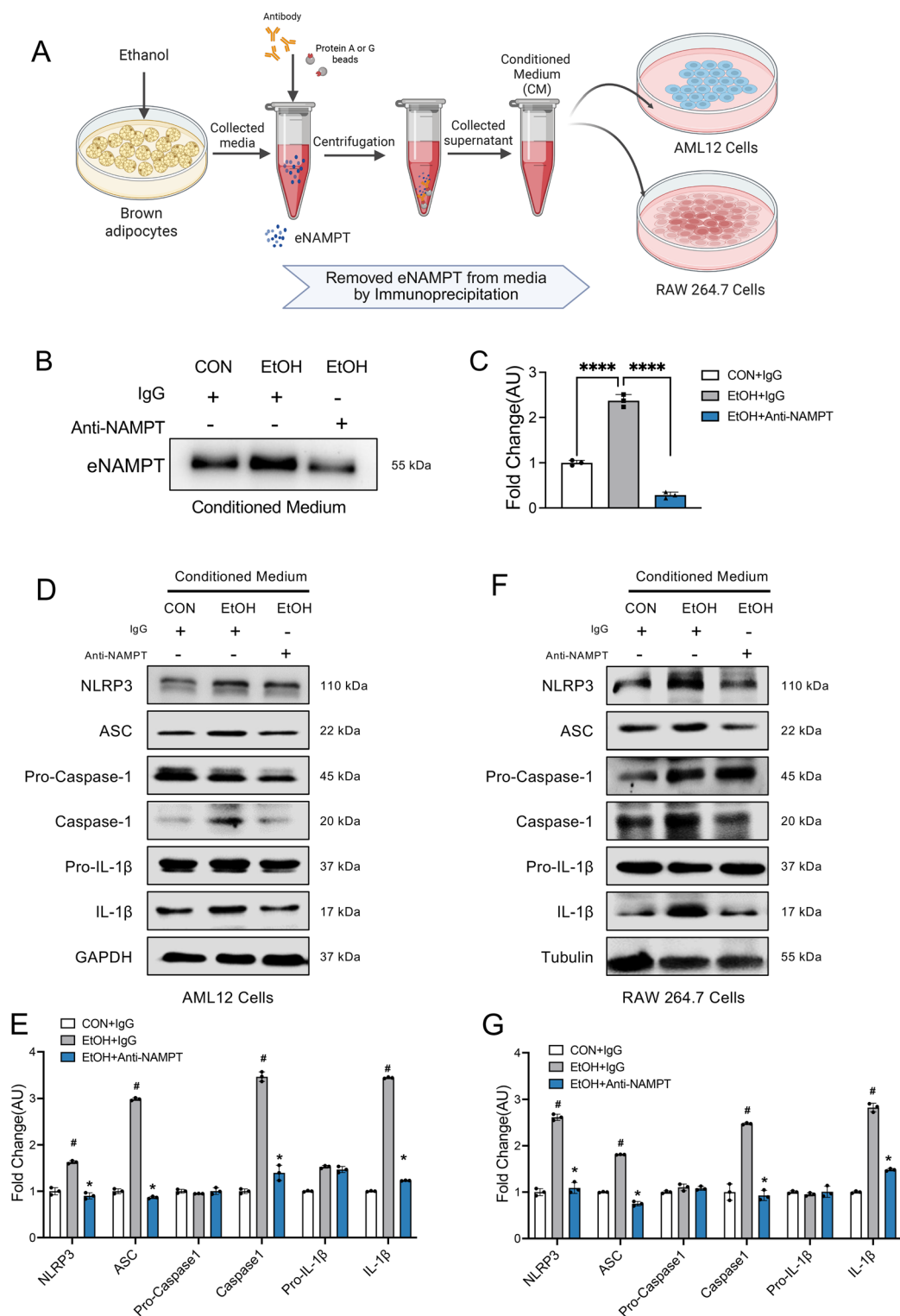


**Fig. 3** BACs-derived eNAMPT induces NLRP3 inflammasome activation in hepatocytes and macrophages. (A) Isolation stromal vascular fraction cells (SVFs) were differentiated to mature brown adipocytes, brown adipocytes were treated with or without EtOH ( $100 \text{ mmol L}^{-1}$ ) for 96 h, the eNAMPT in collected media of brown adipocytes after ethanol intervention was removed by immunoprecipitation with NAMPT-antibody, the conditioned medium (CM) was cultured with AML12 cells and RAW 264.7 cells for 24 h; (B) eNAMPT levels in this CM were detected by western blot, (C) results were expressed as fold changes of control; (D) western blot analysis of NLRP3 inflammasome proteins in AML12 cells, (E) results expressed as fold changes relative to the control; (F) western blot analysis of NLRP3 inflammasome proteins in RAW 264.7 cells, (G) results expressed as fold changes relative to the control. Data are presented as mean (SD). \* $p < 0.05$  compared with the EtOH + IgG group; # $p < 0.05$  compared with the CON + IgG group.



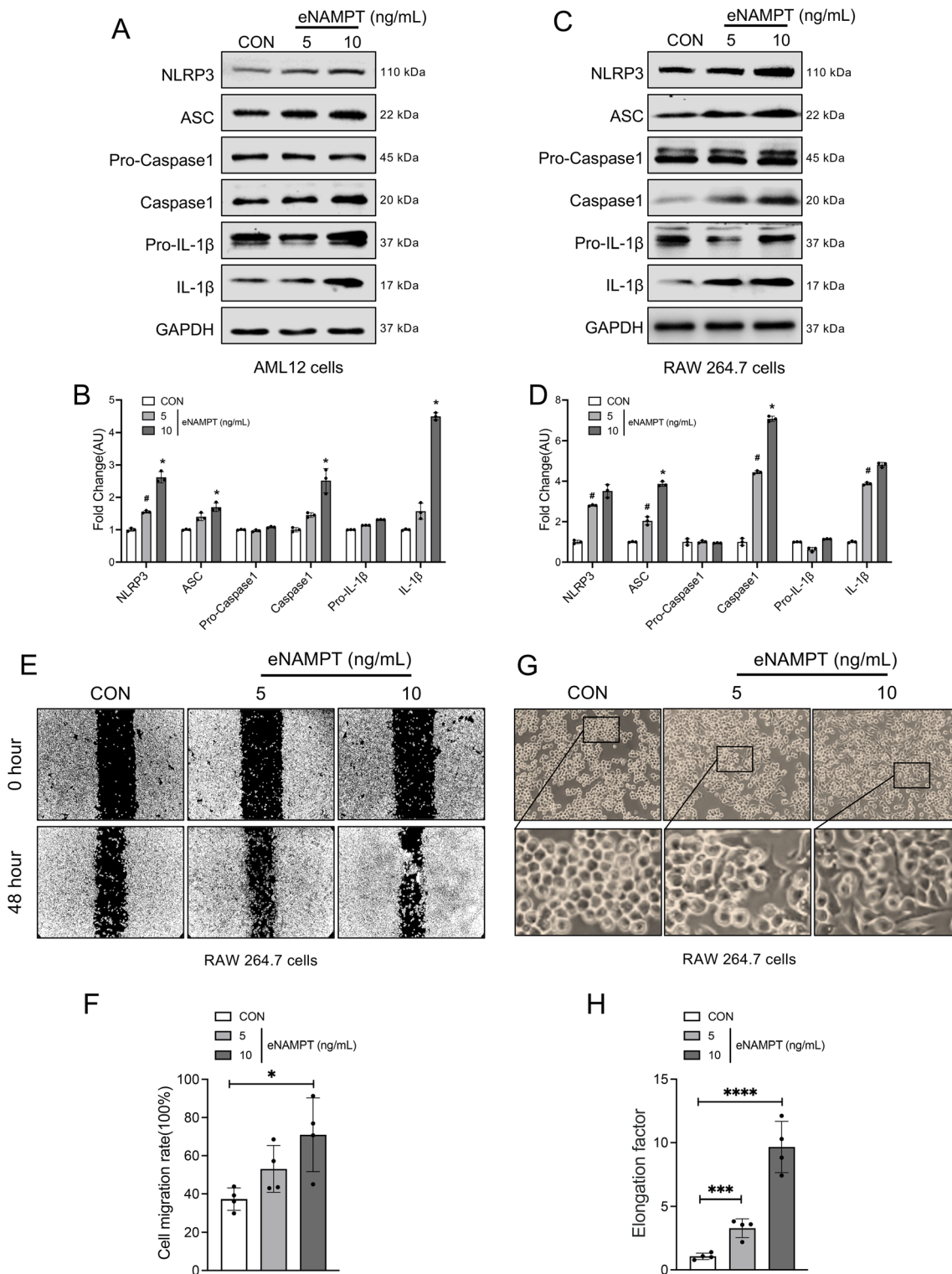


**Fig. 4** Recombinant eNAMPT activates NLRP3 inflammasome in hepatocytes and macrophages. (A–D) AML12 cells and RAW 264.7 cells were incubated with recombinant NAMPT protein (5 ng mL<sup>-1</sup>, 10 ng mL<sup>-1</sup>) for 24 hours, (A) western blot analysis of protein related with NLRP3 inflammasome in AML12 cells, (B) results were expressed as fold changes of control; (C) western blot analysis of protein related with NLRP3 inflammasome in RAW 264.7 cells, (D) results were expressed as fold changes of control. (E) Cell migration of RAW 264.7 cells after incubating with recombinant NAMPT protein (5 ng mL<sup>-1</sup>, 10 ng mL<sup>-1</sup>) for 48 hours; (F) quantitative analysis of cell migration rate. (G) Cell morphological changes of RAW 264.7 cells after incubating with recombinant NAMPT protein (5 ng mL<sup>-1</sup>, 10 ng mL<sup>-1</sup>) for 24 hours; (H) quantitative analysis of cell elongation factor. Data are expressed as mean (SD). \**p* < 0.05 compared with 5 ng mL<sup>-1</sup> eNAMPT treatment; #*p* < 0.05 compared with the control group.



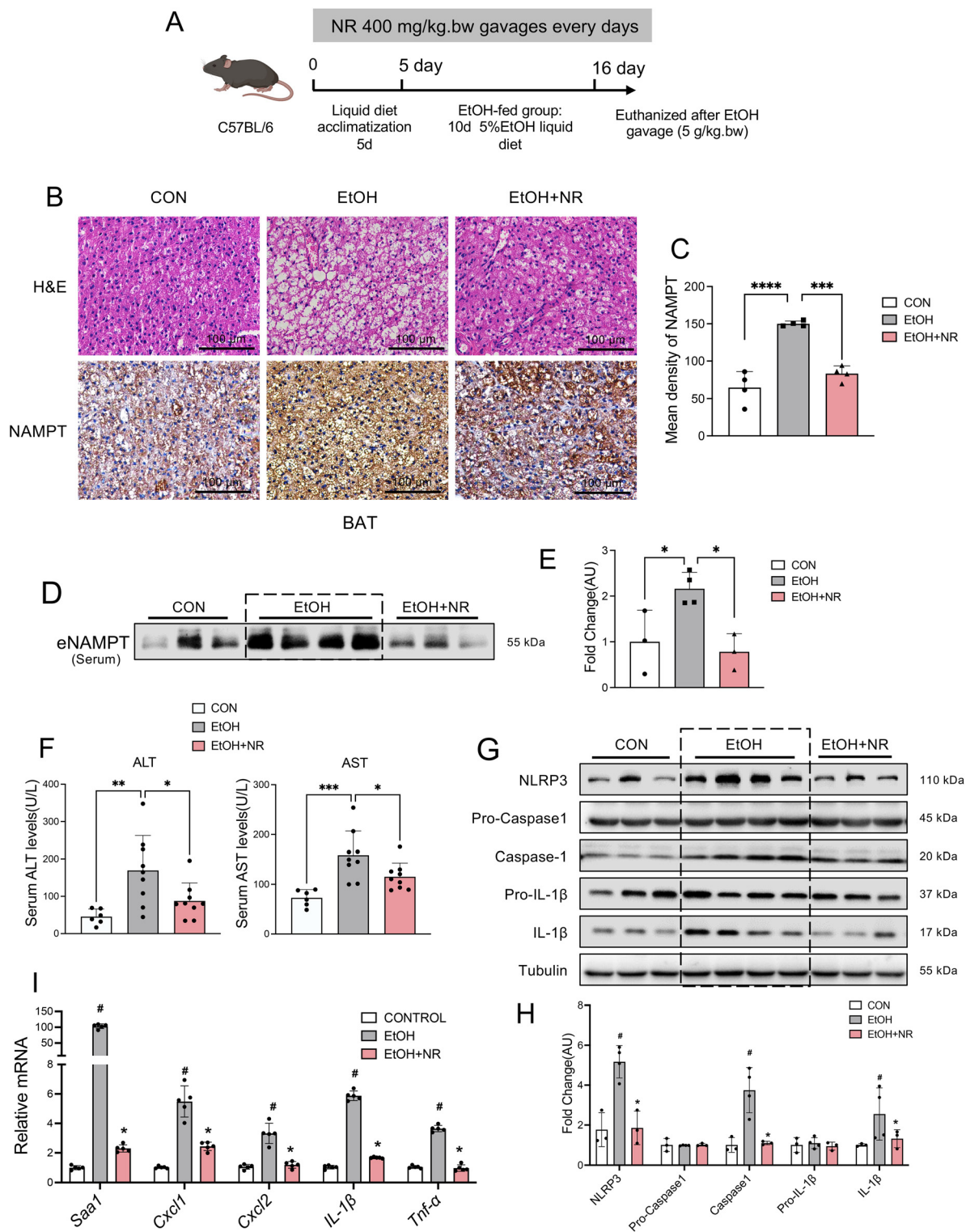


**Fig. 5** NR supplementation decreases circulating eNAMPT levels and protects against alcohol-induced liver NLRP3 inflammasome activation in mice. (A) Schematic of the experimental design of mice were treated with chronic-plus-binge ethanol feeding and nicotinamide riboside (400 mg per kg bw) treatment for 16 days. (B) H&E stain and immunohistochemical staining of NAMPT in mouse BAT. (C) Quantitative analysis of immunohistochemistry. (D) Serum levels of eNAMPT were measured by western blot, (E) results were expressed as fold changes of control. (F) Serum levels of AST and ALT were assessed. (G) Hepatic protein levels of NLRP3 inflammasome were measured by western blot, (H) results were expressed as fold changes of control. (I) Hepatic mRNA levels of pro-inflammatory or anti-inflammatory cytokine genes were measured via qRT-PCR. Data are expressed as mean (SD).  $n = 6-9$  per group,  $**p < 0.01$ ,  $***p < 0.001$ ,  $****p < 0.0001$ ,  $*p < 0.05$  compared with the EtOH group;  $\#p < 0.05$  compared with the control group.



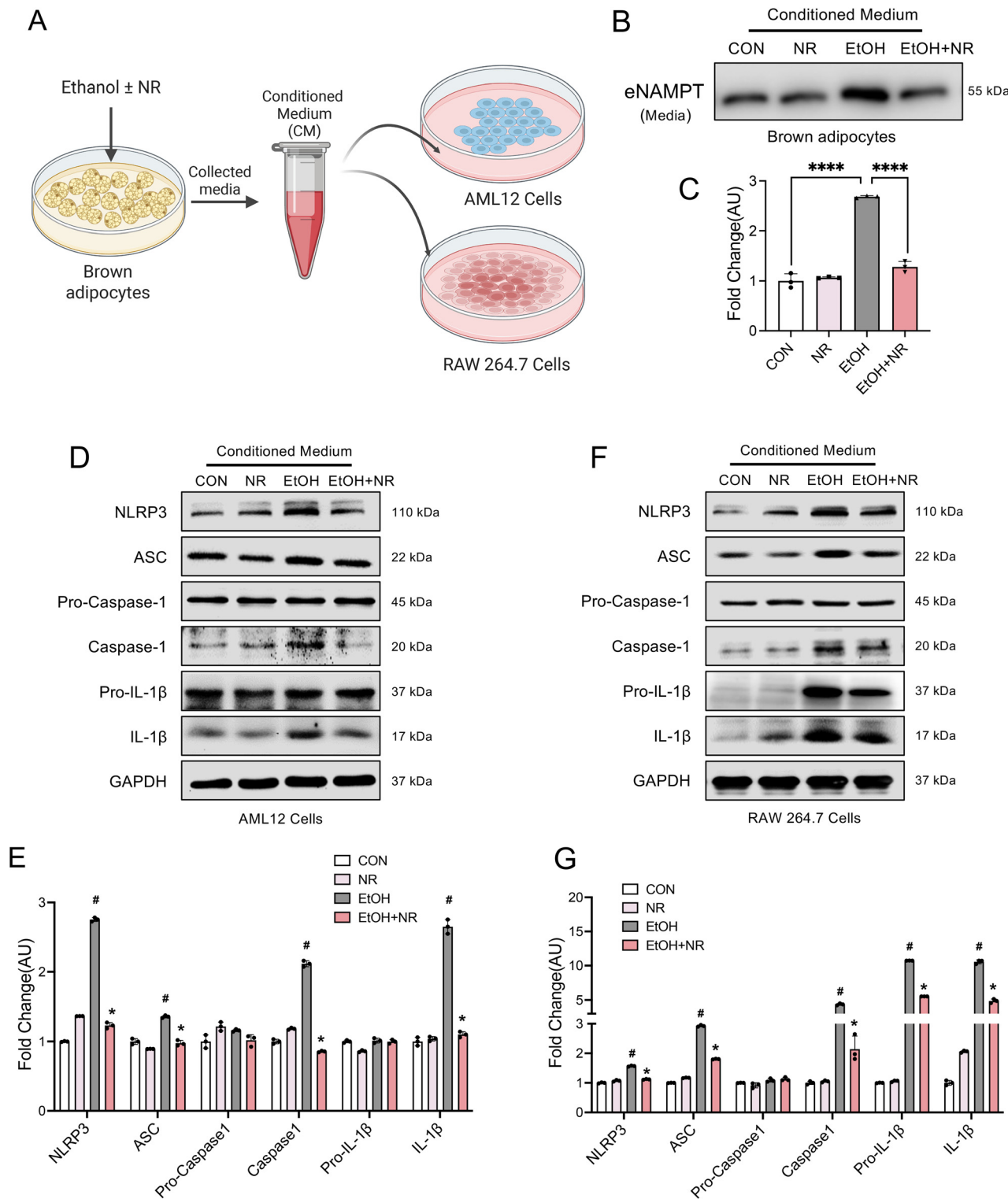


**Fig. 6** NR supplementation inhibits ethanol-induced eNAMPT secretion from BACs. (A and B) brown adipocytes were treated with or without EtOH ( $100 \text{ mmol L}^{-1}$ ) and NR ( $0.5 \text{ mmol L}^{-1}$ ) for 96 h, the media of brown adipocytes after ethanol  $\pm$  NR intervention was collected and cultured with AML12 cells and RAW 264.7 cells for 24 h, (B) western blot analysis of eNAMPT protein expression in cell culture supernatant, (C) results were expressed as fold changes of control. (D) Western blot analysis of NLRP3 inflammasome proteins in AML12 cells, (E) results expressed as fold changes relative to the control; (F) western blot analysis of NLRP3 inflammasome proteins in RAW 264.7 cells, (G) results expressed as fold changes relative to the control. Data are presented as mean (SD). \* $p < 0.05$  compared with the EtOH group; # $p < 0.05$  compared with the CON group.



of caspase-1 and mature IL-1 $\beta$ , resulting in NLRP3 inflammasome activation in AML12 cells (Fig. 6D and E). In contrast, treatment with CM from ethanol + NR significantly reversed these effects (Fig. 6D and E). Similarly, CM from ethanol + NR-treated RAW 264.7 cells suppressed NLRP3 inflammasome activation and reduced IL-1 $\beta$  production compared to CM from ethanol alone (Fig. 6F and G). Additionally, neutralizing eNAMPT in the CM from ethanol + NR can further inhibit NLRP3 expression in BACs (Fig. S7A and B). These results indicate that NR supplementation inhibits ethanol-induced eNAMPT secretion from brown adipocytes, contributing to the inactivation of the NLRP3 inflammasome in AML12 and RAW 264.7 cells.

### 3.7 NR supplementation inhibits hepatic NLRP3 inflammasome activation by suppressing ethanol-induced eNAMPT secretion from BACs

To further verify whether NR supplementation inhibits hepatic NLRP3 inflammasome activation by suppressing ethanol-induced eNAMPT secretion from brown adipocytes, we knocked down NAMPT expression in BACs (Fig. S8A and B). NAMPT-knockdown brown adipocytes were then incubated with ethanol, with or without NR, for 96 hours. The conditioned medium was collected and transferred to AML12 and RAW 264.7 cells for 24 hours (Fig. 7A). As expected, NR supplementation failed to inhibit ethanol-induced eNAMPT secretion from brown adipocytes following NAMPT knockdown (Fig. 7B and C). Then, we assessed the expression of NLRP3 inflammasome-related proteins by western blot. Both AML12 and RAW 264.7 cells demonstrated the same outcome: the CM from ethanol-treated adipocytes with NR intervention inhibited the inflammatory response in hepatocytes and macrophages. However, this protective effect was lost when NAMPT was knocked down in brown adipocytes (Fig. 7D–G). These results suggest that NR can protect against alcohol-induced liver inflammation by inhibiting the secretion of eNAMPT from BACs.

## 4. Discussion

Our study highlights the critical role of eNAMPT secreted from brown adipocytes (BACs) in the pathogenesis of alcoholic liver disease (ALD). We demonstrate that ethanol exposure enhances eNAMPT secretion from BACs, while neutralization of circulating eNAMPT significantly reduces NLRP3 inflammasome activation and the production of proinflammatory cytokines in both *in vivo* and *in vitro*. Moreover, supplementation with nicotinamide riboside (NR), a dietary vitamin B3, suppressed ethanol-induced eNAMPT release and attenuated NLRP3 inflammasome activation, revealing a novel anti-inflammatory effect of NR in ALD. These findings suggest eNAMPT as a promising therapeutic target and highlight NR as a potential nutritional intervention for ALD.

eNAMPT, an adipokine highly expressed in adipose tissue, is secreted during the differentiation of brown adipocytes.<sup>26,27</sup>

Consistent with previous studies, we observed a gradual increase in eNAMPT secretion during BAC maturation, suggesting that adipose tissue is a key contributor to circulating eNAMPT levels. Elevated eNAMPT concentrations have been implicated in metabolic and inflammatory disorders such as atherosclerosis, obesity, type 2 diabetes, and cancer.<sup>28–30</sup> Importantly, serum eNAMPT levels have been shown to increase with chronic alcohol intake.<sup>31</sup> In our study, ethanol promoted eNAMPT secretion both *in vivo* and *in vitro*, and neutralizing eNAMPT with a polyclonal antibody significantly mitigated NLRP3 inflammasome activation. This is in line with reports that eNAMPT-targeting antibodies ameliorate radiation-induced lung fibrosis and septic lung injury,<sup>14,32</sup> and reduce liver damage in nonalcoholic liver disease models.<sup>33</sup> These results collectively suggest that targeting eNAMPT offers broad therapeutic potential across inflammation-related diseases.

Initially identified as a proinflammatory factor in the bone marrow,<sup>34</sup> eNAMPT also functions as a damage-associated molecular pattern (DAMP) and TLR4 ligand, activating the NF- $\kappa$ B signaling pathway.<sup>35</sup> This activation triggers NLRP3 inflammasome assembly and cytokine release.<sup>25</sup> Previous studies have shown that eNAMPT disrupts endothelial integrity and promotes IL-1 $\beta$  secretion *via* NLRP3 activation.<sup>18,36</sup> Our findings confirm that eNAMPT contributes to hepatic inflammation by activating the NLRP3 inflammasome, providing new mechanistic insight into the pathogenic role of eNAMPT in ALD. In addition, we observed that Alexa Fluor 488-labeled recombinant eNAMPT localized on the membrane of RAW 264.7 cells and promoted it to M1 polarization, suggesting that eNAMPT may promote pro-inflammatory macrophage phenotype through receptor-dependent pathways, consistent with previous reports of its interaction with TLR4. Further studies are needed to directly confirm this molecular interaction. In our previous study, we demonstrated that eNAMPT aggravates hepatic injury through promoting hepatocellular ferroptosis, identifying eNAMPT as a key mediator of cell death in ALD.<sup>12</sup> Given the close interplay between ferroptosis and inflammatory signaling<sup>37,38</sup> particularly through the release of DAMPs, we hypothesized that eNAMPT might also contribute to ALD *via* inflammatory pathways. In the present study, we extended our investigation to identify the role of eNAMPT in NLRP3 inflammasome activation. Our findings delineate the multifaceted role of eNAMPT in ALD progression, bridging cell death and inflammation, and highlighting its potential as an upstream regulator and therapeutic target.

Similar studies have demonstrated that eNAMPT exacerbates liver injury, steatosis, hepatitis, and cirrhosis in mice,<sup>15</sup> suggest that eNAMPT may play a significant role in the progression of liver diseases. As liver disease advances to decompensated cirrhosis, liver transplantation often becomes the sole viable treatment option.<sup>2,39</sup> Thus, there is a pressing need to explore effective strategies for the prevention and treatment of ALD before it progresses to cirrhosis. NR is a superior NAD<sup>+</sup> precursor and nutritional supplement with benefits in metabolic and aging-related diseases,<sup>40,41</sup> effectively reduces



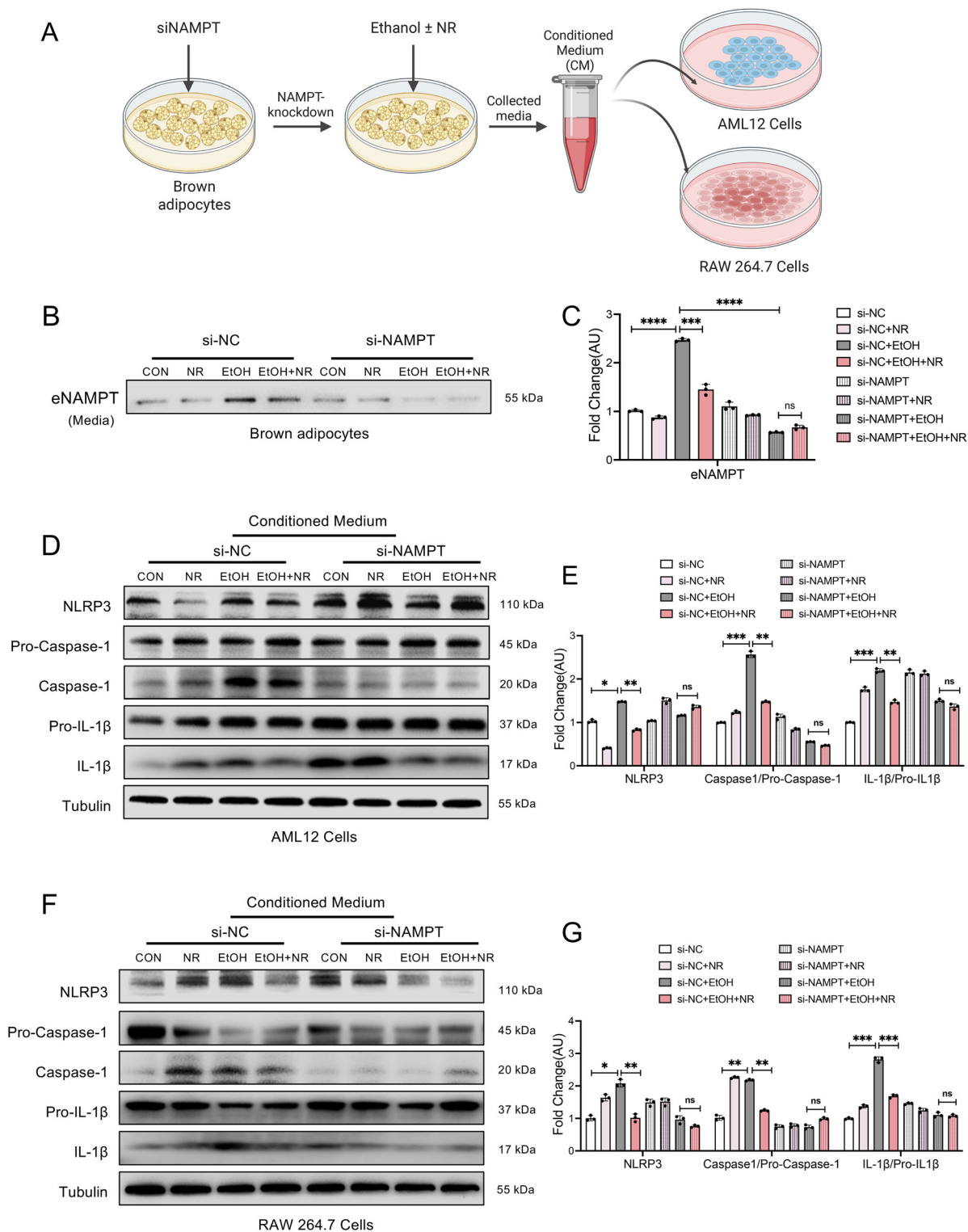


**Fig. 7** NR supplementation inhibits hepatic NLRP3 inflammasome activation by suppressing ethanol-induced eNAMPT secretion from BACs. (A and B) NAMPT-knockdown brown adipocytes were treated with or without EtOH ( $100 \text{ mmol L}^{-1}$ ) and NR ( $0.5 \text{ mmol L}^{-1}$ ) for 96 h, the media of brown adipocytes after ethanol  $\pm$  NR intervention was collected and cultured with AML12 cells and RAW 264.7 cells for 24 h, (B) western blot analysis of eNAMPT protein expression in cell culture supernatant, (C) results were expressed as fold changes of control. (D) Western blot analysis of NLRP3 inflammasome proteins in AML12 cells, (E) results expressed as fold changes relative to the control; (F) western blot analysis of NLRP3 inflammasome proteins in RAW 264.7 cells, (G) results expressed as fold changes relative to the control. Data are presented as mean (SD). \* $p < 0.05$ , \*\* $p < 0.01$ , \*\*\* $p < 0.001$ , \*\*\*\* $p < 0.0001$ .



ethanol-induced eNAMPT secretion from BACs. Previous reports have shown that nicotinamide reduces eNAMPT secretion under stress conditions,<sup>24</sup> and that NAD<sup>+</sup> metabolism is closely tied to eNAMPT production.<sup>42</sup> Consistent with these observations, we found that NR supplementation reduced ethanol-induced intracellular NAMPT expression while restoring intracellular NAD<sup>+</sup> levels in brown adipocytes, further supporting that its protective effects are mediated through modulation of cellular NAD metabolism. Our earlier work found that palmitate-induced eNAMPT secretion could be reversed by cyanidin-3-*O*-glucoside, which also elevated hepatic NAD<sup>+</sup> levels in mice fed high-fat and ethanol-enriched diets.<sup>22,43</sup> These results further support the idea that eNAMPT release is nutritionally regulated and metabolically sensitive.

Mechanistically, NR-mediated inhibition of eNAMPT secretion led to the suppression of NLRP3 inflammasome activation in both hepatocytes and macrophages. Our study mainly demonstrated that NR protects the liver by indirectly suppressing ethanol-induced eNAMPT secretion from brown adipocytes. However, NR may also exert direct protective effects. NR supplementation can increase intracellular NAD<sup>+</sup> availability, thereby enhancing mitochondrial function, promoting oxidative metabolism, and attenuating inflammatory signaling in cardiac hypertrophy,<sup>44</sup> liver inflammation,<sup>45</sup> and neuroinflammation.<sup>46</sup> NR may act through both direct and indirect mechanisms to protect against alcoholic liver injury, suggesting its broad therapeutic potential as a nutritional intervention. Importantly, we show that the protective effect of NR on hepatic inflammation was lost when NAMPT was knocked down in BACs, confirming that its anti-inflammatory efficacy depends on the regulation of BACs-derived eNAMPT. This is a novel mechanism for the protective effect of NR and highlights its potential role as a clinically applicable dietary supplement.

Despite the promising findings, our study has several limitations. The multiple physiological roles of eNAMPT, including intracellular involvement in NAD<sup>+</sup> biosynthesis, make it difficult to selectively block extracellular activity without affecting beneficial functions. Liver inflammation is also regulated by multiple mediators that may compensate for eNAMPT inhibition, and the long-term safety of such interventions remains uncertain. In additions, it is important to acknowledge the differences between mouse models and human alcoholic liver disease. The relative abundance of brown adipose tissue is lower in adult humans compared with mice, which may influence the extent to which BAT-derived eNAMPT contributes to liver inflammation. Even though our study demonstrated the protective effects of NR in mouse models and cell lines, the optimization of dosage and consideration of individual difference are still required in human studies.

## 5. Conclusions

In conclusion, our study identifies BACs-derived eNAMPT as a key upstream driver of NLRP3 inflammasome activation in

alcoholic liver injury. Targeting eNAMPT, either through neutralizing antibodies or NR supplementation, effectively alleviates hepatic inflammation in ALD. These findings support the translational potential of eNAMPT as a therapeutic target and highlight NR as a promising nutritional intervention for the prevention and treatment of ALD.

## Author contributions

Conceptualization, Yujia Zhou and Lili Yang; data curation, Yujia Zhou, Xuye Lai, Nengzhi Pang, Wenli Li, Qiuyan Li and Lei Pei; formal analysis, Nengzhi Pang; funding acquisition, Zhenfeng Zhang and Lili Yang; investigation, Yujia Zhou, Xuye Lai and Nengzhi Pang; methodology, Yujia Zhou, Xuye Lai, Nengzhi Pang, Wenli Li, Qiuyan Li, Jie Pan and Mingtao Chen; project administration, Yujia Zhou, Xuye Lai and Lili Yang; resources, Zhenfeng Zhang; software, Yujia Zhou, Nengzhi Pang and Wenli Li; supervision, Lili Yang, Zhenfeng Zhang; validation, Yujia Zhou, Xuye Lai and Lili Yang; visualization, Yujia Zhou; writing – original draft, Yujia Zhou; writing – review & editing, Lili Yang.

## Conflicts of interest

The authors declare that the research was conducted in the absence of any commercial or financial relationships that could be construed as potential conflicts of interest.

## Institutional review board statement

The animal study protocol was approved by the Animal Care and Utilization Committee of Sun Yat-sen University (2021002133).

## Abbreviations

|                |  |
|----------------|--|
| ALD            | Alcoholic liver disease                                    |
| AML12          | Alpha mouse liver 12                                       |
| ASC            | Apoptosis-associated speck-like protein containing a CARD  |
| BACs           | Brown adipocytes   |
| BAT            | Brown adipose tissue                                       |
| CCL4           | Carbon tetrachloride                                       |
| CM             | Conditioned medium   |
| Cy-3-G         | Cyanidin-3- <i>O</i> - $\beta$ -glucoside                  |
| DAMP           | Damage-associated molecular pattern                        |
| DEGs           | Differentially expressed genes                             |
| eNAMPT         | Extracellular<br>phosphoribosyltransferase<br>nicotinamide |
| IL-1 $\beta$   | Interleukin-1beta  |
| NAD            | Nicotinamide adenine dinucleotide                          |
| NF- $\kappa$ B | Nuclear factor kappa-B                                     |
| NIAAA          | National institute on alcohol abuse and alcoholism         |



|               |   |
|---------------|---|
| NLRP3         | Nucleotide-binding domain-like receptor protein 3 |
| NR            | Nicotinamide riboside                             |
| SIRT1         | Sirtuin 1   |
| TNF- $\alpha$ | Tumor necrosis factor- $\alpha$                   |
| TLR4          | Toll-like receptor 4                              |

## Data availability

The datasets generated during and/or analyzed during the current study are available from the corresponding author upon reasonable request.

The uncropped, full-length Western blot images and supplementary figures are included in SI. See DOI: <https://doi.org/10.1039/d5fo03002a>.

## Acknowledgements

This work was supported by the National Natural Science Foundation of China (grant numbers 81872613 and 82473311).

## References

- 1 F. Åberg, Z. G. Jiang, H. Cortez-Pinto and V. Männistö, Alcohol-associated liver disease-Global epidemiology, *Hepatology*, 2024, **80**, 1307–1322.
- 2 B. H. Mullish and M. R. Thursz, Alcohol-associated liver disease: Emerging therapeutic strategies, *Hepatology*, 2024, **80**, 1372–1389.
- 3 J. Gao, Q. Zheng, F. Y. Lai, C. Gartner, P. Du, Y. Ren, *et al.*, Using wastewater-based epidemiology to estimate consumption of alcohol and nicotine in major cities of China in 2014 and 2016, *Environ. Int.*, 2020, **136**, 105492.
- 4 H. Xu, P. Xiao, F. Zhang, T. Liu and Y. Gao, Epidemic characteristics of alcohol-related liver disease in Asia from 2000 to 2020: A systematic review and meta-analysis, *Liver Int.*, 2022, **42**, 1991–1998.
- 5 K. Sasaki, S. Rooge, S. Gunewardena, J. A. Hintz, P. Ghosh, I. A. Pulido Ruiz, *et al.*, Kupffer cell diversity maintains liver function in alcohol-associated liver disease, *Hepatology*, 2024, **81**, 870–887.
- 6 N. Zhang, H. Zhang, X. Liang, Y. Xu, G. Wang, Y. Bai, *et al.*, Neuroprotective effect of folic acid by maintaining DNA stability and mitochondrial homeostasis through the ATM/CHK2/P53/PGC-1 $\alpha$  pathway in alcohol-exposed mice, *Food Funct.*, 2025, **16**, 4874–4893.
- 7 Y. Liu and M. Chen, Liver-adipose tissue crosstalk in non-alcoholic fatty liver disease: The emerging role of remnant cholesterol, *J. Hepatol.*, 2024, **80**, e111–e112.
- 8 K. A. Sjøberg, C. M. Sigvardsen, A. Alvarado-Diaz, N. R. Andersen, M. Larance, R. J. Seeley, *et al.*, GDF15 increases insulin action in the liver and adipose tissue via a  $\beta$ -adrenergic receptor-mediated mechanism, *Cell Metab.*, 2023, **35**, 1327–1340.
- 9 J. Xu, L. Cui, J. Wang, S. Zheng, H. Zhang, S. Ke, *et al.*, Cold-activated brown fat-derived extracellular vesicle-miR-378a-3p stimulates hepatic gluconeogenesis in male mice, *Nat. Commun.*, 2023, **14**, 5480.
- 10 M. Yoshida, A. Satoh, J. B. Lin, K. F. Mills, Y. Sasaki, N. Rensing, *et al.*, Extracellular Vesicle-Contained eNAMPT Delays Aging and Extends Lifespan in Mice, *Cell Metab.*, 2019, **30**, 329–342.
- 11 F. Carbone, L. Liberale, A. Bonaventura, A. Vecchie, M. Casula, M. Cea, *et al.*, Regulation and Function of Extracellular Nicotinamide Phosphoribosyltransferase/Visfatin, *Compr. Physiol.*, 2017, **7**, 603–621.
- 12 Y. Zhou, N. Pang, W. Li, Q. Li, J. Luo, Y. Gu, *et al.*, Inhibition of ethanol-induced eNAMPT secretion attenuates liver ferroptosis through BAT-Liver communication, *Redox Biol.*, 2024, **75**, 103274.
- 13 J. S. Kim, H. K. Kim, M. Kim, S. Jang, E. Cho, S. J. Mun, *et al.*, Colon-Targeted eNAMPT-Specific Peptide Systems for Treatment of DSS-Induced Acute and Chronic Colitis in Mouse, *Antioxidants*, 2022, **11**, 2376.
- 14 S. Sammani, T. Bermudez, C. L. Kempf, J. H. Song, J. C. Fleming, V. Reyes Herson, *et al.*, eNAMPT Neutralization Preserves Lung Fluid Balance and Reduces Acute Renal Injury in Porcine Sepsis/VILI-Induced Inflammatory Lung Injury, *Front. Physiol.*, 2022, **13**, 916159.
- 15 Y. J. Heo, S. E. Choi, N. Lee, J. Y. Jeon, S. J. Han, D. J. Kim, *et al.*, Visfatin exacerbates hepatic inflammation and fibrosis in a methionine-choline-deficient diet mouse model, *J. Gastroenterol. Hepatol.*, 2021, **36**, 2592–2600.
- 16 S. Paik, J. K. Kim, H. J. Shin, E. J. Park, I. S. Kim and E. K. Jo, Updated insights into the molecular networks for NLRP3 inflammasome activation, *Cell. Mol. Immunol.*, 2025, **22**, 563–596.
- 17 J.-L. Yang, Z.-H. Zhang, X.-L. Jiang, S.-Q. Wang, Y.-L. Wu, J.-X. Nan, *et al.*, Food additive  $\beta$ -caryophyllene mitigates alcoholic steatohepatitis by dual modulation of inflammation and lipid metabolism: a diet-based intervention strategy, *Food Funct.*, 2025, **16**, 5393–5408.
- 18 T. Romacho, I. Valencia, M. Ramos-González, S. Vallejo, M. López-Esteban, O. Lorenzo, *et al.*, Visfatin/eNampt induces endothelial dysfunction in vivo: a role for Toll-Like Receptor 4 and NLRP3 inflammasome, *Sci. Rep.*, 2020, **10**, 5386.
- 19 S. A. Trammell, L. Yu, P. Redpath, M. E. Migaud and C. Brenner, Nicotinamide Riboside Is a Major NAD<sup>+</sup> Precursor Vitamin in Cow Milk, *J. Nutr.*, 2016, **146**, 957–963.
- 20 R. Jiang, Y. Zhou, S. Wang, N. Pang, Y. Huang, M. Ye, *et al.*, Nicotinamide riboside protects against liver fibrosis induced by CCl<sub>4</sub> via regulating the acetylation of Smads signaling pathway, *Life Sci.*, 2019, **225**, 20–28.
- 21 S. Wang, T. Wan, M. Ye, Y. Qiu, L. Pei, R. Jiang, *et al.*, Nicotinamide riboside attenuates alcohol induced liver injuries via activation of SirT1/PGC-1 $\alpha$ /mitochondrial biosynthesis pathway, *Redox Biol.*, 2018, **17**, 89–98.



- 22 L. Pei, T. Wan, S. Wang, M. Ye, Y. Qiu, R. Jiang, *et al.*, Cyanidin-3-O-beta-glucoside regulates the activation and the secretion of adipokines from brown adipose tissue and alleviates diet induced fatty liver, *Biomed. Pharmacother.*, 2018, **105**, 625–632.
- 23 A. Bertola, S. Mathews, S. H. Ki, H. Wang and B. Gao, Mouse model of chronic and binge ethanol feeding (the NIAAA model), *Nat. Protoc.*, 2013, **8**, 627–637.
- 24 M. J. Yoon, M. Yoshida, S. Johnson, A. Takikawa, I. Usui, K. Tobe, *et al.*, SIRT1-Mediated eNAMPT Secretion from Adipose Tissue Regulates Hypothalamic NAD<sup>+</sup> and Function in Mice, *Cell Metab.*, 2015, **21**, 706–717.
- 25 Y. Huang, W. Xu and R. Zhou, NLRP3 inflammasome activation and cell death, *Cell. Mol. Immunol.*, 2021, **18**, 2114–2127.
- 26 J. W. Park, E. Roh, G. M. Kang, S. Y. Gil, H. K. Kim, C. H. Lee, *et al.*, Circulating blood eNAMPT drives the circadian rhythms in locomotor activity and energy expenditure, *Nat. Commun.*, 2023, **14**, 1994.
- 27 N. G. Casanova, J. D. Herazo-Maya, C. L. Kempf, B. L. Sun, J. H. Song, A. Hernandez, *et al.*, eNAMPT Is a Novel DAMP and Therapeutic Target in Human and Murine Pulmonary Fibrosis, *Am. J. Respir. Cell Mol. Biol.*, 2025, DOI: [10.1165/rcmb.2024-0342OC](https://doi.org/10.1165/rcmb.2024-0342OC).
- 28 L. Gao, F. J. Ramirez, J. T. O. Cabrera, M. V. Varghese, M. Watanabe, A. Tsuji-Hosokawa, *et al.*, eNAMPT is a novel therapeutic target for mitigation of coronary microvascular disease in type 2 diabetes, *Diabetologia*, 2024, **67**, 1998–2011.
- 29 L. Zhang, L. Wang, Z. Xu, X. Zhang, S. Guan, Z. Liu, *et al.*, eNAMPT/Ac-STAT3/DIRAS2 Axis Promotes Development and Cancer Stemness in Triple-Negative Breast Cancer by Enhancing Cytokine Crosstalk Between Tumor-Associated Macrophages and Cancer Cells, *Int. J. Biol. Sci.*, 2025, **21**, 2027–2047.
- 30 M. Rodriguez, H. Xu, A. Hernandez, J. Ingraham, J. Canizales, F. T. Arce, *et al.*, NEDD4 E3 ligase-catalyzed NAMPT ubiquitination and autophagy activation are essential for pyroptosis-independent NAMPT secretion in human monocytes, *Cell Commun. Signaling*, 2025, **23**, 157.
- 31 H. C. Yu, S. Y. Li, M. F. Cao, X. Y. Jiang, L. Feng, J. J. Zhao, *et al.*, Effects of chronic ethanol consumption on levels of adipokines in visceral adipose tissues and sera of rats, *Acta Pharmacol. Sin.*, 2010, **31**, 461–469.
- 32 A. N. Garcia, N. G. Casanova, C. L. Kempf, T. Bermudez, D. G. Valera, J. H. Song, *et al.*, eNAMPT Is a Novel Damage-associated Molecular Pattern Protein That Contributes to the Severity of Radiation-induced Lung Fibrosis, *Am. J. Respir. Cell Mol. Biol.*, 2022, **66**, 497–509.
- 33 B. L. Sun, X. Sun, C. L. Kempf, J. H. Song, N. G. Casanova, S. M. Camp, *et al.*, Involvement of eNAMPT/TLR4 inflammatory signaling in progression of non-alcoholic fatty liver disease, steatohepatitis, and fibrosis, *FASEB J.*, 2023, **37**, e22825.
- 34 B. Samal, Y. Sun, G. Stearns, C. Xie, S. Suggs and I. McNiece, Cloning and characterization of the cDNA encoding a novel human pre-B-cell colony-enhancing factor, *Mol. Cell. Biol.*, 1994, **14**, 1431–1437.
- 35 M. Gasparrini, F. Mazzola, M. Cuccioloni, L. Sorci, V. Audrito, F. Zamporlini, *et al.*, Molecular insights into the interaction between human nicotinamide phosphoribosyltransferase and Toll-like receptor 4, *J. Biol. Chem.*, 2022, **298**, 101669.
- 36 A. N. Garcia, N. G. Casanova, D. G. Valera, X. Sun, J. H. Song, C. L. Kempf, *et al.*, Involvement of eNAMPT/TLR4 signaling in murine radiation pneumonitis: protection by eNAMPT neutralization, *Transl. Res.*, 2022, **239**, 44–57.
- 37 M. Mu, C. X. Huang, C. Qu, P. L. Li, X. N. Wu, W. Yao, *et al.*, Targeting Ferroptosis-Elicited Inflammation Suppresses Hepatocellular Carcinoma Metastasis and Enhances Sorafenib Efficacy, *Cancer Res.*, 2024, **84**, 841–854.
- 38 U. Gupta, S. Ghosh, C. T. Wallace, P. Shang, Y. Xin, A. P. Nair, *et al.*, Increased LCN2 (lipocalin 2) in the RPE decreases autophagy and activates inflammasome-ferroptosis processes in a mouse model of dry AMD, *Autophagy*, 2023, **19**, 92–111.
- 39 M. Israelsen, W. Rungratanawanich, M. Thiele and S. Liangpunsakul, Non-invasive tests for alcohol-associated liver disease, *Hepatology*, 2024, **80**, 1390–1407.
- 40 W. I. Ryu, M. Shen, Y. Lee, R. A. Healy, M. K. Bormann, B. M. Cohen, *et al.*, Nicotinamide riboside and caffeine partially restore diminished NAD availability but not altered energy metabolism in Alzheimer's disease, *Aging Cell*, 2022, **21**, e13658.
- 41 W. S. Song, X. Shen, K. Du, C. B. Ramirez, S. H. Park, Y. Cao, *et al.*, Nicotinic acid riboside maintains NAD(+) homeostasis and ameliorates aging-associated NAD(+) decline, *Cell Metab.*, 2025, **37**, 1499–1514.
- 42 L. Morató, S. Astori, I. Zalachoras, J. Rodrigues, S. Ghosal, W. Huang, *et al.*, eNAMPT actions through nucleus accumbens NAD(+)/SIRT1 link increased adiposity with sociability deficits programmed by peripuberty stress, *Sci. Adv.*, 2022, **8**, eabj9109.
- 43 Y. Zhou, S. Wang, T. Wan, Y. Huang, N. Pang, X. Jiang, *et al.*, Cyanidin-3-O-beta-glucoside inactivates NLRP3 inflammasome and alleviates alcoholic steatohepatitis via SirT1/NF-kappaB signaling pathway, *Free Radical Biol. Med.*, 2020, **160**, 334–341.
- 44 S. Ma, J. Feng, X. Lin, J. Liu, Y. Tang, S. Nie, *et al.*, Nicotinamide Riboside Alleviates Cardiac Dysfunction and Remodeling in Pressure Overload Cardiac Hypertrophy, *Oxid. Med. Cell. Longevity*, 2021, **2021**, 5546867.
- 45 R. W. Dellinger, H. E. Holmes, T. Hu-Seliger, R. W. Butt, S. A. Harrison, D. Mozaffarian, *et al.*, Nicotinamide riboside and pterostilbene reduces markers of hepatic inflammation in NAFLD: A double-blind, placebo-controlled clinical trial, *Hepatology*, 2023, **78**, 863–877.
- 46 Y. Hou, Y. Wei, S. Lautrup, B. Yang, Y. Wang, S. Cordonnier, *et al.*, NAD(+) supplementation reduces neuroinflammation and cell senescence in a transgenic mouse model of Alzheimer's disease via cGAS-STING, *Proc. Natl. Acad. Sci. U. S. A.*, 2021, **118**, e2011226118.

